Demonstration of focusing by a neutron accelerator

Yasushi Arimoto
High Energy Accelerator Research Organization, Tsukuba, Ibaraki 305-0801, Japan

Peter Gertenbort
Institut Laue-Langevin, Boîte Postale 156, F-38042 Grenoble Cedex 9, France

Sohei Imajo
Department of Physics, Kyoto University, Kitashirakawa, Kyoto 606-8502, Japan

Yoshihisa Iwashita
Institute of Cemical Research, Kyoto University, Uji, Kyoto 611-0011, Japan

Masaaki Kitaguchi*
Research Reactor Institute, Kyoto University, Kumatori, Osaka 590-0494, Japan

Yoshichika Seki
RIKEN, Wako, Saitama 351-0198, Japan

Hirohiko M. Shimizu
Department of Physics, Nagoya University, Chikusa, Nagoya 464-8602, Japan

Tamaki Yoshioka
Department of Physics, Kyushu University, Hakozaki, Fukuoka 812-8581, Japan
(Received 23 May 2012; published 23 August 2012)

Space-time focusing was demonstrated by a neutron accelerator. Test experiments were performed by using very slow neutrons at High-Flux Reactor at Institut Laue-Langevin. Focusing of neutrons at the detector position through the accelerator was observed. Focusing neutrons enables us to transport the neutrons while maintaining density from source to experimental position. This will be a powerful technique for measurement of the permanent electric dipole moment of neutrons, which require a high density of neutrons.

DOI: 10.1103/PhysRevA.86.023843 PACS number(s): 37.20.+j, 28.20.Gd, 29.27.Eg

I. INTRODUCTION

The permanent electric dipole moment of neutrons (NEDM) signals the violation of time-reversal T invariance. Although experimental searches have been pursued in the world [1–5], the NEDM has not yet been observed. The present upper limit is $|d_n| < 2.9 \times 10^{-26}\, e\,\mathrm{cm}$ (90% C.L.) [5], which is very close to the predictions of some physics beyond the standard model of particle physics, for example, supersymmetry. For improvement of experimental sensitivity, the density of neutrons is quite important in order to reduce the systematic errors from the uncertainty of the environment. We are now developing the transport system against loss of neutron density.

In the case of a pulsed neutron source, the neutrons, which are generated as a pulse with high density instantaneously, spread spatially and lose density during transport because of their velocity distribution. When fast neutrons are decelerated and/or slow neutrons are accelerated properly in the middle of the transport, these neutrons can be focused on the experimental area at the same time while recovering the density (Fig. 1) [6–9].

II. NEUTRON ACCELERATOR FOR FOCUSING

For the acceleration or deceleration of neutrons, we can utilize flipping of neutron spin in the magnetic field. The energy change of the neutron by using rf and a static magnetic field under the resonance condition has been already observed [10,11]. Although this change is too small to be used for the focusing of fast neutrons, it is enough to realize the focusing with very slow neutrons. Such slow neutrons that have a kinetic energy of less than about 200 neV, called ultracold neutrons (UCNs), are used in NEDM experiments. In this demonstration we use the adiabatic fast passage (AFP) method, which is one of the spin flippers [12]. When a neutron passes through an rf magnetic field in the surrounding static field with smooth gradient, the neutron's spin flips with an energy gain or loss corresponding to the spin polarization. The change of the neutron kinetic energy is written as $2\mu B$, where B is the magnetic field at the spin-flip position and μ is magnetic dipole moment of the neutron. After the magnetic field, the velocity becomes $\sqrt{v^2 \pm 2\mu B/m}$ from the incident velocity of v, where

*kitaguch@rri.kyoto-u.ac.jp

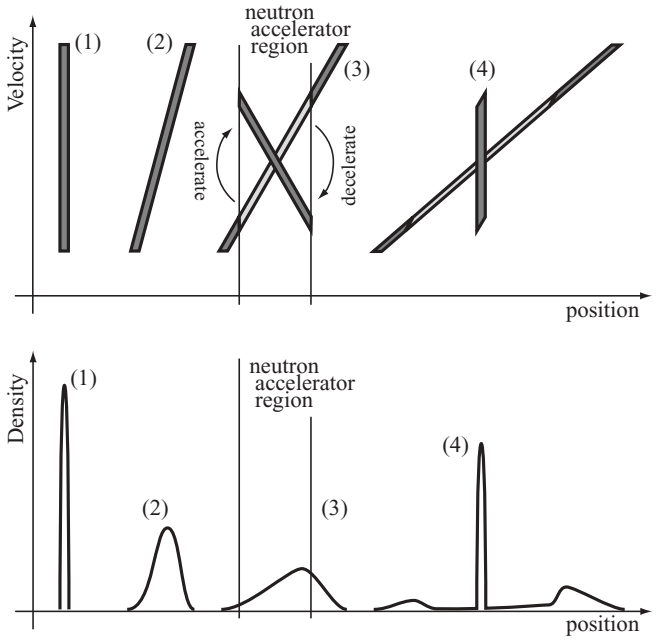

FIG. 1. Concept of space-time focusing by using a neutron accelerator. (1) Neutrons are generated as a pulse. (2) Neutrons spread spatially during transport. (3) Neutrons are accelerated or decelerated properly. (4) Some neutrons are focused at the experimental position. This figure illustrates the behavior of polarized neutrons.

m is the neutron mass and the plus-minus sign represents gain and loss of the energy. In the case of deceleration, the time of flight of a neutron with the initial velocity v is written as

$$T = \int_0^{L_f} \sqrt{\frac{m}{2[E_0 - \mu B(z)]}}\,dz + \int_{L_f}^{L} \sqrt{\frac{m}{2[E_0 - 2\mu B(L_f) + \mu B(z)]}}\,dz, \qquad (1)$$

where L_f is the spin-flip position, L is the detector position, and $E_0 = mv^2/2$ is initial kinetic energy of the neutron. When we select L_f for each velocity of the neutron properly, the time of flight can be kept constant. Because the spin flip occurs under the resonance condition, which is written as $\hbar\omega = 2\mu B(L_f)$, where ω is the frequency of the rf field, changing the frequency can be utilized to select the spin-flip position. There is a time lag for arriving at the spin-flip position for each velocity; therefore, the frequency is represented as a function of time $\omega(t)$, which can be calculated numerically by Eq. (1) when T and $B(z)$ are given. The AFP spin flipper with time-changing rf frequency is required for focusing of neutrons.

III. EXPERIMENTS AND RESULTS

We made the AFP spin flipper the neutron accelerator, which consists of a compact static magnet to generate the gradient field with 1 T at the maximum and an rf coil to generate the resonance rf field. The magnet has anisotropic interpoles in order to generate a homogeneous gradient of the magnetic field in the direction of neutron beam [13,14]. The strength of the field decreases from 1 to 0.5 T in 20 cm. The

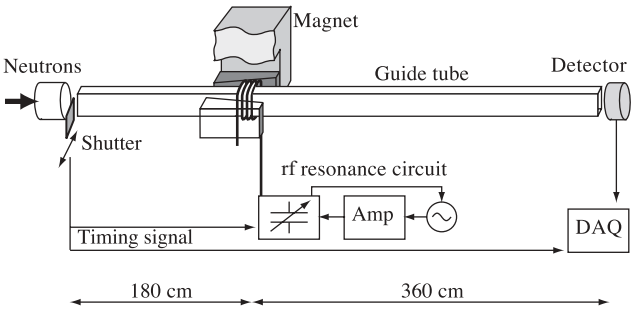

FIG. 2. Experimental setup. The neutron accelerator is installed in the middle of the guide tube. The rf and data acquisition systems are synchronized with the shutter operation.

rf coil has a length of 20 cm, which covers the gradient of the static field. The rf can be modulated automatically from 30 to 15 MHz by using electric circuits with variable capacitors and a signal generator. The control of the capacitors selects the spin-flip position L_f, which can be synchronized with the neutron pulse. The rf power is supplied by a wideband amplifier with 1-kW output.

The space-time focusing experiment was performed at the PF2 TES beamline in the High-Flux Reactor at Institut Laue-Langevin. The whole experimental setup is shown in Fig. 2. Very slow neutrons including UCNs were provided from the turbine, which decelerates the neutrons from the reactor by using continuous reflections off rotating mirrors [15]. The neutrons had the velocity distribution shown in Fig. 3. A mechanical shutter is used to supply pulsed neutrons. The shutter opened for 20 ms once every 2 s. A neutron-absorbing cadmium pipe is inserted just before the shutter in order to reduce the number of reflections by limiting the neutron divergence. A neutron detector, which is a ^{3}He gas detector, is set 5.6 m downstream from the shutter. The neutrons were transported with reflections off the mirror inside the guide tube. The size of the guide is 6 cm vertical and 3 cm horizontal. The guide consists of assembled glass plates with nickel coating, which has high reflectivity for neutrons. For the neutrons with a velocity of less than 7 m/s, which are used in NEDM experiments, the reflectivity is estimated at higher than 99%. The transport efficiency of the guide tube was 92% after reflections of 43 times on average. Since we are going to

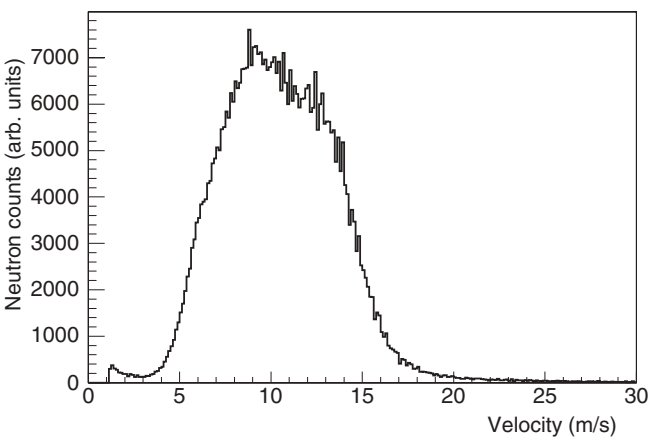

FIG. 3. Measured velocity distribution of incident neutrons.

accelerate or decelerate neutron velocity only in the transport direction, nonspecular reflection at the guide surface should be suppressed as much as possible. The glass plates were polished and aligned parallel enough to keep the velocity in the transport direction. The measurements of the neutron velocity distribution through the guide tube were consistent with the simulations without nonspecular reflections at the surfaces. The static magnet and rf coil were arranged midway between the shutter and the detector. The rf coil was wound to the guide tube.

We measured the time-of-flight (TOF) spectrum of the neutrons through this setup for two cases: The rf was on and off. The static magnetic field is constantly applied throughout the experiments. In the case of the rf off, the spins of the neutrons are not flipped and the net velocities are not changed before and after the static magnet. In the case of the rf on, the rf field is applied only when neutrons with velocity from 5.7 to 5.0 m/s reach the accelerator position. This caused the partial change of the shape of the TOF spectrum, which enables us to easily compare the case of the rf on to that of the rf off. In the arrival time lag of 80 ms between the neutrons of the velocity range, the frequency of the rf is swept from 28.6 to 17.5 MHz, which correspond to 120 and 70 neV of the energy exchange, respectively. For this demonstration, the variable capacitor was moved with a constant speed as the approximation of the frequency function $\omega(t)$. A schematic diagram of neutron position, the shutter aperture, and the rf is shown in Fig. 4. The measurement time was about 4 h for both cases. The measured TOF spectra are shown in Fig. 5. The top and bottom histograms represent the cases of the rf off and on, respectively. The lines show the Monte Carlo simulations with and without focusing. The nonspecular reflections at the guide surfaces are not considered in these simulations. For rf-on case, the line is calculated with a spin-flip efficiency of 0.5. Both of the observed histograms are in good agreement with the simulations. The ratio of these two histograms is shown in Fig. 6. The decelerated neutrons focused at the time between 1.2 and 1.4 s can be seen. The loss of constant energy makes only a diffused spectrum and cannot make the excess indicated in the figure.

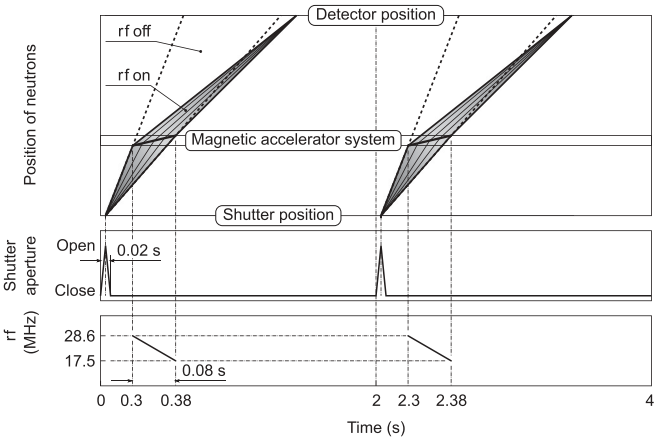

FIG. 4. Position distribution of the neutrons (top). Shutter and rf operation (middle and bottom). Neutrons that are not affected by the accelerator are omitted in this figure. This figure is not to scale.

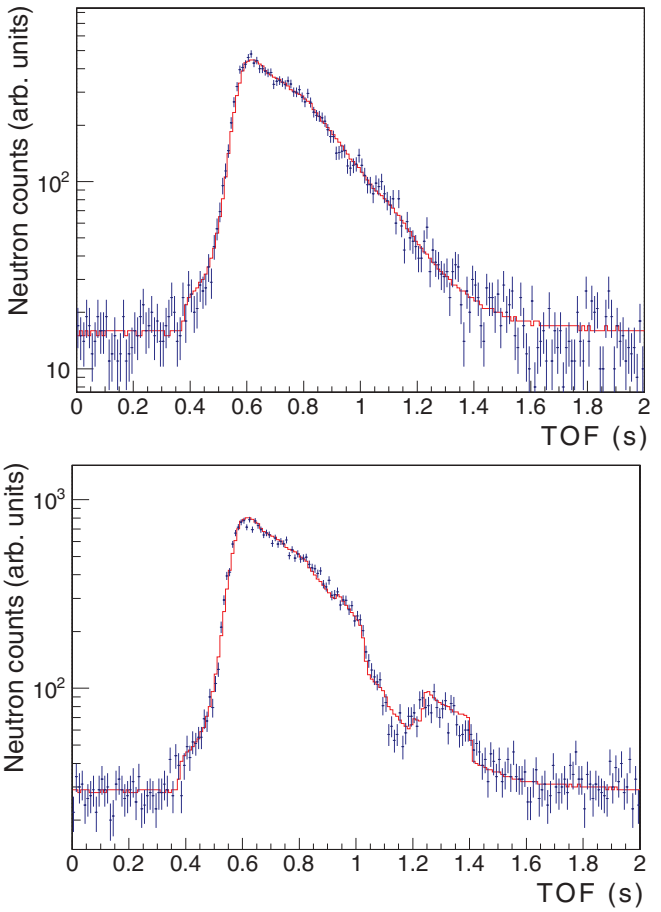

FIG. 5. (Color online) Neutron TOF spectra. Top and bottom show the cases of the rf off and on, respectively. Lines show the simulations.

IV. CONCLUSION

We have successfully developed a neutron magnetic accelerator and demonstrated neutron space-time focusing for transport of UCNs while maintaining density. The results are in good agreement with simple simulations that control the velocities of the neutrons. The efficiency of the spin flip was

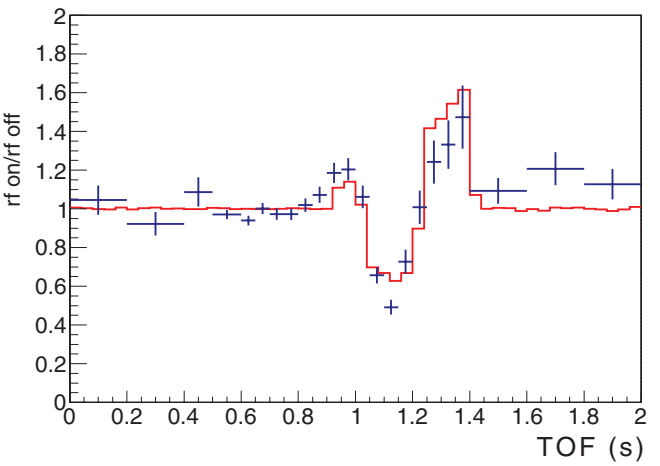

FIG. 6. (Color online) Ratio of these two TOF histograms. Line shows the simulation with focusing.

low; however, this can be improved with the amplitude of the rf field.

This result shows the feasibility of effective transport of UCNs for various experiments. The neutrons can be gathered only in the experimental area at the focus time. When a shutter at the entrance of the experimental area closes just after the injection of the focused pulse, the UCNs can be localized only in the experimental area with high density without spreading in the guide tubes. The combination of this device and a highly instantaneously intense pulsed source, for example, the Spallation Neutron Source and Japan Proton Accelerator Complex, enables us to utilize neutrons most effectively. It should be mentioned that the excitation current of our magnet and its stray field is constant during the experiment, in contrast to the method mentioned in Ref. [8]. This is fairly advantageous to NEDM experiments, which require extremely precise magnetic field control. The constant excitation of the magnet eases a quick modulation of the accelerating energy. In addition, since this device can manipulate the longitudinal phase space distribution of the neutrons flexibly, it can adjust not only the time structure but also the energy distribution, as suggested in Refs. [6,7]. These features widen the application of this system.

ACKNOWLEDGMENTS

We would like to thank T. Brenner for the intensive and helpful assistance during the experiment. This work was supported by the Grants-in-Aid for Scientific Research of the Ministry of Education of Japanese Government under the Programs No. 19GS0210 and No. 23244047; the Quantum Beam Fundamentals Development Program of the Ministry of Education, Culture, Sports, Science and Technology; and Yamada Science Foundation.

[1] J. Simith, E. M. Purcell, and N. F. Ramsey, Phys. Rev. **108**, 120 (1957).
[2] W. B. Dress, P. D. Miller, J. M. Pendlebury, P. Perrin, and N. F. Ramsey, Phys. Rev. D **15**, 9 (1977).
[3] K. F. Smith *et al.*, Phys. Lett. B **234**, 191 (1990).
[4] I. S. Altarev *et al.*, Phys. Lett. B **276**, 242 (1992).
[5] C. A. Baker *et al.*, Phys. Rev. Lett. **97**, 131801 (2006).
[6] J. Summhammer, L. Niel, and H. Rauch, Z. Phys. B **62**, 269 (1986).
[7] L. Niel and H. Rauch, Z. Phys. B **74**, 133 (1989).
[8] A. I. Frank and R. Gähler, Phys. At. Nucl. **63**, 545 (2000).
[9] H. M. Shimizu, Y. Iwashita, M. Kitaguchi, K. Mishima, and T. Yoshioka, Nucl. Instrum. Methods Phys. Res. A **634**, 55 (2011).
[10] B. Alefeld, G. Badurek, and H. Rauch, Z. Phys. B **41**, 231 (1981).
[11] H. Weinfurter *et al.*, Z. Phys. B **72**, 195 (1988).
[12] A. Abragam, *Principles of Nuclear Magnetism* (Oxford University Press, Oxford, 1961).
[13] Y. Arimoto *et al.*, Phys. Procedia **17**, 20 (2011).
[14] Y. Arimoto *et al.*, IEEE Trans. Appl. Supercond. **22**, 4500704 (2012).
[15] A. Steyerl *et al.*, Phys. Lett. A **116**, 347 (1986).